Published in final edited form as:
Genesis. 2013 October ; 51(10): 677–689. doi:10.1002/dvg.22416.

The *Ptch1*^{DL} mouse: a new model to study lambdoid craniosynostosis and basal cell nevus syndrome associated skeletal defects

Weiguo Feng[1,&], **Irene Choi**[1], **David E. Clouthier**[1], **Lee Niswander**[2], and **Trevor Williams**[1,#]

[1]Department of Craniofacial Biology and Cell and Developmental Biology, University of Colorado Anschutz Medical Campus, 12801 East 17th Avenue, Aurora, CO 80045

[2]Department of Pediatrics, Howard Hughes Medical Institute, University of Colorado Anschutz Medical Campus, 12801 East 17th Avenue, Aurora, CO 80045

Abstract

Mouse models provide valuable opportunities for probing the underlying pathology of human birth defects. Employing an ENU-based screen for recessive mutations affecting craniofacial anatomy we isolated a mouse strain, *Dogface-like* (*DL*), with abnormal skull and snout morphology. Examination of the skull indicated that these mice developed craniosynostosis of the lambdoid suture. Further analysis revealed skeletal defects related to the pathology of basal cell nevus syndrome (BCNS) including defects in development of the limbs, scapula, ribcage, secondary palate, cranial base, and cranial vault. In humans, BCNS is often associated with mutations in the Hedgehog receptor *PTCH1* and genetic mapping in *DL* identified a point mutation at a splice donor site in *Ptch1*. Using genetic complementation analysis we determined that *DL* is a hypomorphic allele of *Ptch1*, leading to increased Hedgehog signaling. Two aberrant transcripts are generated by the mutated *Ptch1*^{DL} gene, which would be predicted to reduce significantly the levels of functional Patched1 protein. This new *Ptch1* allele broadens the mouse genetic reagents available to study the Hedgehog pathway and provides a valuable means to study the underlying skeletal abnormalities in BCNS. In addition, these results strengthen the connection between elevated Hedgehog signaling and craniosynostosis.

Keywords

Hedgehog; Craniosynostosis; Polydactyly; Craniofacial Defects; Omphalocele

Introduction

Forward genetic screens in mice have yielded considerable insight into the genetics underlying the molecular mechanisms responsible for normal development (Caspary and Anderson, 2006). In particular, *N*-ethyl-*N*-nitrosourea (ENU) mutagenesis has provided an effective means to introduce a high frequency of random point mutations into the mouse genome. Subsequently, phenotype-driven dominant and recessive screens, coupled with mapping and high-throughput sequencing approaches, have provided an unbiased means to identify novel genes critical for multiple aspects of development. Even in instances where

[#]Corresponding author: Trevor Williams, Department of Craniofacial Biology and Cell and Developmental Biology, University of Colorado Denver, Mailstop 8120, 12801 East 17th Avenue, Aurora, CO 80045. 303-724-4571 – telephone 303-724-4580 – fax Trevor.Williams@ucdenver.edu.
[&]Current address: Cancer Institute and Institute for Stem Cell Biology and Regenerative Medicine, Stanford University School of Medicine, Stanford, CA 94305

the mutation maps to a gene previously linked to a developmental pathway, these ENU-induced mutations can yield new alleles that can provide valuable information on gene function during development.

We recently conducted a recessive ENU screen focused on identifying mutations altering the morphology of the craniofacial skeleton. In humans, birth defects affecting the head, face and oral tissues are frequent dysmorphologies with severe medical consequences (Gritli-Linde, 2008). While clefting of the lip and/or palate are common defects, there are many other syndromic and non-syndromic conditions that alter the shape and growth of the face and skull. One notable human facial defect, bossing of the forehead, is a feature of Basal Cell Nevus Syndrome (BCNS), previously termed Gorlin Syndrome (Evans and Farndon, 2010). BCNS is a dominantly inherited condition caused by mutations in one allele of *PTCH1*, the gene encoding the transmembrane receptor and negative regulator of the Hedgehog (Hh) signaling pathway (Lindstrom *et al.*, 2006; Quijada *et al.*, 2006; Robbins *et al.*, 2012; Wicking *et al.*, 1997). Many aspects of BCNS manifest during childhood and into adulthood, including basal cell carcinomas, nevi, palmar and plantar pits, jaw keratocysts, and medulloblastoma (Evans and Farndon, 2010; Kimonis *et al.*, 1997; Kimonis *et al.*, 2013; Lo Muzio, 2008). In addition, there are several notable congenital defects associated with the head and orofacial complex including macrocephaly, mandibular prognathism, coronoid hyperplasia, hyperpneumatization of the sphenoid, bridging of the sella turcica, high arched palate and occasional orofacial clefting (Evans and Farndon, 2010; Iwanaga *et al.*, 1998; Kimonis *et al.*, 1997; Kimonis *et al.*, 2013; Lo Muzio, 2008). Skeletal defects in the trunk affect the sternum and ribcage, the shoulder, the vertebrae, and the limbs, the latter typified by syndactyly and polydactyly.

Studies using the mouse model system have provided insight into the function of the Ptch1 protein in development as well as in the etiology of BCNS. *Ptch1*-null mice die around embryonic day 9 (E9) and have neural tube closure defects (Goodrich *et al.*, 1997; Hahn *et al.*, 1998). Conditional *Ptch1* gene knockout analyses have also been employed to study bone development and physiology and have indicated important roles for *Ptch1* in formation of the long bones and calvaria, and in bone homeostasis (Mak *et al.*, 2008; Mak *et al.*, 2006) as well as in patterning the limb bud (Bruce *et al.*, 2010; Butterfield *et al.*, 2009). *Ptch1* heterozygous mice develop problems associated with BCNS including medulloblastoma and basal cell carcinoma (Goodrich *et al.*, 1997; Hahn *et al.*, 1998). Additionally, such mice show variable defects associated with aberrant embryogenesis including large size, syndactyly and polydactyly as well as accelerated osteogenesis that affects pre- and post-natal bone formation (Goodrich *et al.*, 1997; Hahn *et al.*, 1998; Ohba *et al.*, 2008). Despite the various models that can be utilized to study *Ptch1* function in the mouse, analyses focused on development of the craniofacial skeleton relevant to BCNS are hampered by early embryonic lethality and exencephaly (Butterfield *et al.*, 2009; Goodrich *et al.*, 1997; Hahn *et al.*, 1998; Milenkovic *et al.*, 1999; Ngan *et al.*, 2011). Here we describe the isolation and characterization of a new ENU-induced recessive mouse model, $Ptch1^{DL}$ that displays many of the skeletal hallmarks of BCNS. This mutation adds a valuable new hypomorphic allele of *Ptch1* that can be used to assess the role of the Hh signaling pathway in multiple developmental events, particularly those regulating facial shape in both a clinical and evolutionary context (Roberts *et al.*, 2011).

Results

Identification of the *Dogface-like* (*DL*) mutant

We used ENU-treated founder C57BL/6J male mice and a three-generation cross to conduct a recessive screen to identify mutations that affect late embryonic development, focusing in part on the embryonic day 18.5 (E18.5) craniofacial skeleton. From this, we identified a

mutant line that we termed *DL* (*Dogface-like*) in which ∼25% of the offspring from heterozygous matings were larger than their littermates and displayed a more rounded skull with an abnormal angle between the cranium and the snout (Figure 1a, b). Examination of the external morphology indicated that these mice also exhibited preaxial polydactyly associated with all four limbs (Figure 1d and Table 1). When mice were allowed to develop to term, the mutant animals did not survive until weaning.

Skeletal staining of affected E18.5 mutants showed features apparent in the intact embryos, such as the domed cranial vault along with the aberrant angle between this region and the snout in lateral view compared with controls (Figure 2a, b). Additionally, dorsal views of *Ptch1*^{DL} mutant skulls revealed large areas lacking skeletal components in regions where the bones of the skull vault normally juxtapose, particularly near the midline (Figure 2c, d red arrows). Ventral views of the skull (Figure 2e-h) showed defects of the cranial base, especially in components of the sphenoid bone. Notably, the presphenoid was absent, the basisphenoid was narrower along its rostral caudal axis, and the alisphenoids were hypoplastic. The palatal shelves were underdeveloped compared to wild-type and were absent in ∼10% of mutants in association with a cleft secondary palate (2/15 embryos). Examination of the mandible indicated that the coronoid process also failed to extend caudally (Figure 2j). Surprisingly, despite the apparent hypoplastic or perhaps delayed intramembranous ossification of the frontal, parietal and interparietal bones near the midline, there were consistent defects associated with the sutures. In particular, the lambdoid sutures, between the parietal and interparietal bones, were consistently malformed (Figure 2l). Whereas there was a gap present between these two bones in control embryos, *Ptch1*^{DL} mutants showed consistent fusion of these two bones, especially towards the more ventral aspect of the skull, so that they became contiguous regions of ossification. Defects in suture formation were less apparent for other calvarial bones at this stage of development, and in comparison to the parietal and interparietal bones, such bones could readily be teased apart with fine forceps. Finally, interfrontal bone ossification was often seen at the rostral portion of the calvaria, associated with the abnormally wide distance between the two frontal bones (T. Williams, data not shown).

Examination of the trunk and appendicular skeleton revealed additional defects in *Ptch1*^{DL} mice. The sternum was disorganized with irregular ossification associated with asymmetric insertion of individual pairs of ribs in all mutants examined (Figure 3a, b). The manubrium and xiphoid process were also thicker and/or irregular. Examination of the *Ptch1*^{DL} scapulas showed that these were mostly normal, although one contained a large central foramen (Figure 3c, d). In addition, limb skeletons confirmed the underlying skeletal defects associated with preaxial polydactyly (Figure 3e-h). All hindlimbs examined had six digits, whereas the forelimbs were more variable, sometimes possessing six or seven digits but more often having an abnormally broad or syndactylous first digit.

DL corresponds to a point mutation in *Ptch1*

The ENU-mutagenized C57BL/6J founder male was outcrossed onto a wild type 129S1/SvImJ background, as were subsequent generations. The mutant phenotype has remained fairly consistent despite the change in genetic background. Meiotic recombination mapping enabled the approximate position of the mutation to be identified using polymorphic markers that distinguished between these two mouse strains. Initially, using markers spanning ∼10 mega base pair (Mb) intervals throughout the mouse autosomes, the mutation was mapped to an ∼12 Mb region on chromosome 13 (between polymorphic markers D13Mit13 and D13Mit 281). Subsequently, markers D13Mit283 and D13Mit 311 were used to refine the position of the mutation. Inspection of the ∼350,000 bp interval indicated that it contained *Ptch1*, encoding a receptor for Hedgehog ligands, a gene known to be responsible

for controlling body size, limb patterning and bone development (Bruce *et al.*, 2010; Goodrich *et al.*, 1997; Hahn *et al.*, 1998; Mak *et al.*, 2008; Mak *et al.*, 2006; Makino *et al.*, 2001; Milenkovic *et al.*, 1999; Ohba *et al.*, 2008; Sweet *et al.*, 1996). Therefore, *Ptch1* genomic DNA from $Ptch1^{DL}$ mutants was sequenced and this revealed a single nucleotide change at the 3′-end of exon 13. This mutation altered a guanine present in all wild-type controls to an adenine in all $Ptch1^{DL}$ mice (arrow in Figure 4a). This nucleotide change is located within the splice donor sequence for exon 13, and would change the consensus sequence AG/GT to AAGT. Therefore, RT-PCR was performed to determine if *Ptch1* mRNA splicing was altered in the $Ptch1^{DL}$ mutants. When primers located in *Ptch1* exons 12 and 15 were employed for amplification of control RNA samples the expected 759-base pair (bp) product was generated (Figure 4b). However, $Ptch1^{DL}$ mutant RNA samples generated two PCR products: an abundant band shorter than the control and a weaker band that was a similar size as the control. Sequencing of the shorter $Ptch1^{DL\text{-}b}$ cDNA product demonstrated that it lacked 119 bp of the wild-type transcript due to skipping of exon 13. As a result of the aberrant joining of exon 12 to exon 14 there is a frame shift resulting in a premature stop codon 9 amino acids into the exon 14 sequence (see Figure 4 legend for sequence information). This alteration would result in a significantly truncated Ptch1 protein, $Ptch1^{\text{DL-b}}$, lacking ∼870 C-terminal amino acids required for Hedgehog interaction and signal transduction (Figure 4c). This short product is presumably functionally inactive given these significant alterations. Sequence analysis of the longer $Ptch1^{DL\text{-}a}$ cDNA product also showed that this cDNA was mis-spliced despite its similar size to the control. In this instance, there was read-through across the normal position of splicing at the end of exon 13, with the cDNA continuing into the adjacent intron for an extra 36 bp before a cryptic splice donor sequence, GGGT, was used to splice to exon 14. This alteration would result in a *Ptch1* protein, $Ptch1^{DL\text{-}a}$, which would have an in-frame insertion of 12 amino acids that would be situated in the largest intracellular loop of the protein (Figure 4c; see Figure 4 legend for sequence information). Since the $Ptch1^{DL}$ homozygous embryos survive longer than *Ptch1*-null mice, we predict that the protein encoded by the $Ptch1^{DL\text{-}a}$ transcript retains some functionality in the Hedgehog signal transduction pathway.

Allelic complementation studies demonstrate *DL* is an allele of *Ptch1*

The assignment of *DL* mutation to the *Ptch1* locus was tested using a complementation analysis using two *Ptch1* null alleles. The first allele, $Ptch1^{tm1Zim}$ (Hahn *et al.*, 1998), has a deletion of exons 6 and 7, and the second, *Ptch1-LacZ* ($Ptch1^{tm1Mps}$), has a knock-in of the *LacZ* reporter into exon 2 (Goodrich *et al.*, 1997). Following mating of $Ptch1^{DL}$ and *Ptch1* heterozygous mice, we isolated embryos at E18.5 and performed gross morphological analysis, skeletal staining and genotype analysis. Mice carrying one $Ptch1^{DL}$ allele and either of the *Ptch1* null alleles were morphologically distinct from their littermates. $Ptch1^{tm1Zim}$ and *Ptch1-LacZ* gave similar results in this assay, although there was some variability in the severity of the mutant phenotype for both null alleles (Figures 5, 6 Table 1, and data not shown). At E18.5, viable mice with one $Ptch1^{DL}$ allele and one *Ptch1* null allele were larger than their littermates and had a domed skull with distinct angular separation from the snout (Figure 5). Mice often had kinked tails and a small omphalocele, a body wall closure defect in which several loops of the gut enclosed in amniotic sac occurred outside the body cavity (Figure 5). All mutant mice also had pre-axial polydacytly of the forelimbs and hindlimbs (Figure 6). Several embryos presented with the neural tube closure defect exencephaly, while other mutants failed to develop and were dead upon collection at E18.5 (Table 1 and data not shown). Examination of the craniofacial skeleton in mutant mice with normal neural tube closure revealed similar defects as seen in $Ptch1^{DL}$ homozygous mice (Figure 6). Dorsal views of the skull revealed a major defect in the formation of the endochondrial bones of the calvaria, which was more severe than in homozygous $Ptch1^{DL}$ embryos (Figure 6d). There was also consistent fusion of the parietal

and interparietal bones with absence of the intervening lambdoid suture (black arrow). Ventral views revealed absence of the presphenoid, a narrow basisphenoid, and hypoplasia of the alisphenoid. The palatal shelves were also underdeveloped (Figure 6f) as was the coronoid process of the mandible (Figure 6h). In the trunk, the sternum of *Ptch1*^{DL}*/Ptch1-LacZ* mice was disorganized, thicker and more ossified than littermates (Figure 6j). There was a higher incidence of a foramen present in the scapula than in *Ptch1*^{DL} homozygotes (5/10) and preaxial polydactyly and/or syndactyly was observed for all forelimbs and the majority of hindlimbs (Figure 6l and data not shown). In contrast, none of the control mice presented with these axial or appendicular skeletal defects. The genetic non-complementation observed between the *Ptch1*^{DL} allele and either of the *Ptch1*-null alleles confirmed that *Ptch1*^{DL} was a novel mutant allele for *Ptch1*. Moreover, previous studies have demonstrated that mice lacking *Ptch1* die around E9.5 (Goodrich *et al.*, 1997; Hahn *et al.*, 1998). Therefore, since the homozygous *Ptch1*^{DL} mice and *Ptch1*^{DL}*/Ptch1-null* survive until E18.5, the *Ptch1*^{DL} allele must be hypomorphic and produce sufficient functional Ptch1 protein to rescue the early developmental defects that result from the complete loss of *Ptch1*.

Discussion

Previous sequence analyses of BCNS patients have identified multiple mutations that map to *PTCH1* (Lindstrom *et al.*, 2006; Quijada *et al.*, 2006; Wicking *et al.*, 1997). These types of mutations are concentrated in the N-terminal cytoplasmic region, the two large extracellular loops and the large intracellular loop. A majority of these mutations would be predicted to function as null alleles as they introduce premature nonsense codons causing significant truncations of the protein. Although there are over 100 different *PTCH1* mutations associated with BCNS, to date there has been no evidence of any genotype-phenotype correlations. Here, we describe the identification of a new hypomorphic allele of *Ptch1*, *Ptch1*^{DL}, which was isolated in an ENU-based screen for recessive mouse mutations affecting craniofacial morphology. The splice site mutation present in the *Ptch1*^{DL} allele produces two mutant forms of the protein. The more prevalent *Ptch1* DL-b transcript would produce a significantly truncated protein, with a disruption of the sterol sensing domain (Lindstrom *et al.*, 2006) and loss of all further C-terminal regions. This form would be similar to at least one of the human mutations identified to date. The remaining DL-a transcripts would introduce an additional 12 amino acids into the large intracellular loop of the protein. This loop interacts with cyclin B1 and may function in *Ptch1*-mediated regulation of cell cycle progression (Barnes *et al.*, 2001). However, since *Ptch1*^{DL} homozygous and *Ptch1*^{DL}*/Ptch1*^{null} trans-heterozygotes live until birth, compared to the death of *Ptch1*-homozygous null animals around E9.5, the amount and function of the DL-a protein must be sufficient to fulfill critical aspects of early *Ptch1* function.

Further support for essential levels of functional Ptch1 protein in *Ptch1*^{DL} mutants is also suggested by an examination of heterozygous *Ptch1*^{DL} animals. To date, we have not noted general overgrowth, brain tumors, or limb abnormalities in these mice (data not shown) compared to the occurrence of such phenotypes in some of the *Ptch1*^{null} heterozygous strains (Goodrich *et al.*, 1997; Hahn *et al.*, 1998). At the same time, we note that abnormal heterozygous phenotypes have not been consistently reported, and that genetic background can have a large influence over the phenotypes associated with *Ptch1* mutations (Ellis *et al.*, 2003; Wakabayashi *et al.*, 2007). *Ptch1*^{DL} does appear to be a stronger recessive allele than the previously identified *Ptch1*^{mes} mutation (Makino *et al.*, 2001; Sweet *et al.*, 1996). This latter allele arose spontaneously, and is caused by a 32nt deletion resulting in loss of the last 200 amino acids from the C-terminal intracellular tail of Ptch1 and its replacement by a novel 68 amino acid region following the frame-shift (Makino *et al.*, 2001). In contrast to *Ptch1*^{DL} homozygous mice, *Ptch1*^{mes} homozygous mice are viable, although they have similar defects in the shape of the skull, and the patterning of the sternum and limbs (Sweet

et al., 1996). Further, the $Ptch1^{DL}/Ptch1^{null}$ mice have a stronger cranial base phenotype than trans-heterozygous $Ptch1^{mes}/Ptch1^{null}$ mice. Both allelic combinations die at birth, are larger in size compared to control littermates, and exhibit polydactyly of all four limbs (Makino *et al.*, 2001). However, unlike in $Ptch1^{DL}/Ptch1^{null}$ mice, skeletal staining of $Ptch1^{mes}/Ptch1^{null}$ embryos reveals that the sphenoid is of normal size, the presphenoid is present, and there is a long coronoid process associated with the dentary (data not shown). The $Ptch1^{DL}$ allele therefore provides a valuable new resource to study the function of *Ptch1* in many developmental processes.

In this report, we have focused on the skeletal defects observed in $Ptch1^{DL}$ homozygous embryos and $Ptch1^{DL}/Ptch1^{null}$ trans-heterozygotes. The phenotype of these animals provides mouse models to understand aspects of BCNS that influence the shape of the craniofacial complex, the ribcage, the shoulders, and the limbs (Evans and Farndon, 2010; Iwanaga *et al.*, 1998; Kimonis *et al.*, 1997; Kimonis *et al.*, 2013; Leonardi *et al.*, 2002; Lo Muzio, 2008). Both $Ptch1^{DL}$–based mouse models display preaxial polydactyly, foramens of the scapula, and sternal dysmorphology. In the head, the prominent domed skull shape, similar to the forehead bossing in BCNS patients, may result from a combination of defective cranial base formation and hypoplastic development of the calvaria. Overt clefting of the secondary palate was uncommon in these allelic combinations, but the delayed and/or hypoplastic development of the palatal shelves may be linked to the high arched palate phenotype present in BCNS patients. The defects of the skeletal components that will eventually fuse to form the mature sphenoid bone is also intriguing given the observation of defects in the sella turcica and hyperpneumatization of the sphenoid reported in BCNS (Iwanaga *et al.*, 1998). However, the morphology of the mandible appears to differ significantly between the mouse and human conditions. In particular, there is no clear prognathism in the mouse, and the coronoid process of the dentary is hypoplastic in the mouse models in contrast to the reports of hyperplasia of this structure in human (Leonardi *et al.*, 2002). We hypothesize that these differences reflect either species-specific arrangements of the craniofacial skeleton or discrepancies in the age at which these structures were examined between these two species. Nevertheless, the observed prognathism and coronoid pathology in human, coupled with the coronoid hypoplasia in the $Ptch1^{DL}$ embryos, indicates that reduction of *Ptch1* expression can have profound affects on the shape of the jaw and it's joints.

The $Ptch1^{DL}$ mutant is also relevant in understanding how other alterations in the Hedgehog signaling pathway, including ciliopathies, influence skeletal development and patterning. In this regard, aberrant Hedgehog signaling may underlie some instances of human craniosynostosis, a condition more commonly associated with defects in the Fgf pathway (Holmes, 2012; Klopocki *et al.*, 2011; Yuksel-Apak *et al.*, 2012). The strongest association is with *RAB23*, a negative regulator of Hedgehog signaling that is mutated in Carpenter Syndrome, a condition that includes synostosis of the metopic and sagittal sutures (Jenkins *et al.*, 2007). Two reports have documented craniosynostosis in patients with large chromosomal duplications or deletions in the vicinity of *IHH* that are postulated to cause ectopic expression of this gene (Klopocki *et al.*, 2011; Yuksel-Apak *et al.*, 2012). Lastly, in rare instances, inappropriate fusion of the midline sutures can also occur in Grieg cephalopolysyndactyly, which is caused by mutations in *GLI3*, a transcription factor which acts downstream of *PTCH1* to repress Hedgehog signaling (Hurst *et al.*, 2011). However, analysis of how Hedgehog pathway genes influence craniosynostosis in the mouse has been complicated by exencephaly, early lethality and the function of such genes in ossification of the calvaria (Goodrich *et al.*, 1997; Hahn *et al.*, 1998; Rice *et al.*, 2010; St-Jacques *et al.*, 1999). The function of *Ihh* in intramembranous ossification has been controversial, with reports indicating that both loss and gain of *Ihh* function can cause hypoplastic cranial bone development (Abzhanov *et al.*, 2007; Lenton *et al.*, 2011; St-Jacques *et al.*, 1999). We note

that previous studies targeting *Ptch1* function in chondrocytes, osteoblasts and osteocytes resulted in similar defects in formation and maintenance of the calvaria as observed in Ihh^{null} skulls (Mak *et al.*, 2008; Mak *et al.*, 2006; St-Jacques *et al.*, 1999). Therefore it may be that normal development of the bones of the skull vault requires a critical range of Hedgehog activity. Nevertheless, the failure of the skull bones to juxtapose at the midline in mouse models that exhibit either increased or decreased Hedgehog activity has made it difficult to assess how the genes in this network impact craniosynostosis. One exception has been the $Gli3^{Xt\text{-}J/Xt\text{-}J}$ mouse model that displays lambdoid suture craniosynostosis (Rice *et al.*, 2010). We find that the $Ptch^{DL}$ models exhibit similar premature fusion of the parietal and interparietal bones towards the ventral side of the skull. These findings are consistent with the expression of *Ptch1* in the osteogenic fronts of the calvaria, coincident with *Ihh*, *Gli3* and *Runx2* (Mak *et al.*, 2008; Rice *et al.*, 2010). Further analysis will be required to determine if the juxtaposition of other calvarial bones, particularly at the coronal suture, will result in synostosis in $Ptch^{DL}$ mice. We note that the regions of the parietal and interparietal bones involved in suture formation are both derived from the mesoderm, whereas other bones involved in suture formation have at least one neural crest component (Jiang *et al.*, 2002). Therefore, the embryonic origin of the lambdoid suture could also render it more sensitive to Hedgehog signaling levels. Taken together, though, the findings from the $Gli3^{Xt\text{-}J/Xt\text{-}J}$ and $Ptch1^{DL}$ indicate that a reduction of these two Hedgehog pathway inhibitors both result in lambdoid suture craniosynostsis. Furthermore, our findings raise the possibility that examples of human craniosynostosis could result from alterations in *PTCH1* and that a degree of premature suture fusion may occur in BCNS.

Overall, the phenotypes we observe in $Ptch^{DL}$ embryos are likely caused by a combination of reduced repression of molecular pathways regulated by both Shh and Ihh signaling. Loss of repression of the Hedgehog pathway downstream of *Ihh* likely causes ossification defects in the calvaria, sternum and scapula. With respect to the Hedgehog pathway, similar scapula and sternal defects are present in the $Gli3^{Xt\text{-}J/Xt\text{-}J}$ mouse model as seen with the $Ptch1^{DL}$ embryos (Johnson, 1967; Kuijper *et al.*, 2005). A second link between the Hedgehog pathway and defects in the scapula comes from the examination of the *Doublefoot* (*Dbf*) mouse model (Hayes *et al.*, 1998). Mice heterozygous for *Dbf* have polydactyly and scapula foramina, as well as defects in ossification of the calvaria (Hayes *et al.*, 1998). Subsequent studies indicated that *Ihh* was ectopically expressed in the developing limbs and branchial arches of *Dbf* embryos as a result of a large chromosomal deletion in the vicinity of this gene (Babbs *et al.*, 2008; Yang *et al.*, 1998). In contrast, the polydactyly and syndactyly apparent in $Ptch1^{DL}$ homozygous or $Ptch1^{DL}/Ptch1^{null}$ mice presumably result from deregulation of Shh signaling. We also predict that excess Shh signaling is responsible for the omphalocele observed in the $Ptch1^{DL}$ background, given the presence of this body wall defect in *Gli3* mutants and its rescue by lowering Shh levels in this genetic background (Matsumaru *et al.*, 2011). Despite the anticipated activation of the Hedgehog signaling pathway, our preliminary examination of the $Ptch1^{DL}$/*Ptch1-LacZ* limbs has not shown an expansion of β-galactosidase expression, a readout of activation of *Ptch1* transcription (data not shown). We therefore postulate that levels of functional Ptch1 protein required for this feedback loop to be activated must be lower than present in the $Ptch1^{DL}/Ptch1^{null}$ mice.

With respect to the alteration of the skeletal elements of the cranial base, aberrant responses to both Shh and Ihh are likely involved in the defects seen in $Ptch1^{DL}$ homozygous and $Ptch1^{DL}/Ptch1^{null}$ embryos (Balczerski *et al.*, 2012; McBratney-Owen *et al.*, 2008; Young *et al.*, 2006). The cranial base is derived from both mesodermal and neural crest derivatives with the basisphenoid bone acting as a boundary in association with the rostral extent of the notochord. The notochord acts as a source of Shh and disruption of either Shh or Ihh can alter the development of the cranial base (Balczerski *et al.*, 2012; Nagayama *et al.*, 2008; St-Jacques *et al.*, 1999; Young *et al.*, 2006). Moreover, genetic manipulations that increase Hh

signaling, including mice with *Mks1* or *Tmem107* mutations as well as a K14-Shh transgene, produce similar defects in the cranial base to the *Ptch1*^{DL} mutants (Christopher *et al.*, 2012; Cobourne *et al.*, 2009; Cui *et al.*, 2011; Weatherbee *et al.*, 2009). *Mks1* and *Tmem107* mutants, which affect primary cilia function, also have comparable limb and sternal defects to the *Ptch1*^{DL} mice, reinforcing the connection of these skeletal defects to ciliopathy and increased Hedgehog signaling (Christopher *et al.*, 2012; Cui *et al.*, 2011; Weatherbee *et al.*, 2009). Finally, note that other genetic changes are also associated with loss, reduction or alteration of the presphenoid and basisphenoid bones including mutations in components of the Fgf, Wnt/β-catenin and TGF-β signaling pathways (Caparros-Martin *et al.*, 2013; Dudas *et al.*, 2006; Mai *et al.*, 2010; Meester-Smoor *et al.*, 2005; Nagayama *et al.*, 2008; Pacheco *et al.*, 2012; Reid *et al.*, 2011; Winnier *et al.*, 1997). Determining how these signal transduction pathways and their transcriptional effectors are integrated to control cranial base development will be important to understand the regulation of human facial morphology. In conclusion, the *Ptch1*^{DL} allele adds a valuable new resource to probe the molecular control of development and patterning, especially with respect to the craniofacial skeleton.

Materials and Methods

Mice

Male C57BL/6J mice treated with ENU were kindly provided by Monica Justice (Baylor College of Medicine). Additional C57BL/6J mice, as well as 129S1/SvImJ, *Ptch1*^{tm1Mps}/J (*Ptch1-LacZ*), and B6C3Fe *a/a-Ptch1*^{mes}/J (*Ptch1*^{mes}) were obtained from the Jackson Laboratory (Goodrich *et al.*, 1997; Sweet *et al.*, 1996). B6.129-Ptch1^{tm1Zim}/Cnrm mice (Hahn *et al.*, 1998) were obtained from Emma (The European Mouse Mutant Archive). This study was carried out in strict accordance with the recommendations in the Guide for the Care and Use of Laboratory Animals of the National Institutes of Health. The protocol was approved by the Institutional Animal Care and Use Committee of the University of Colorado Denver. The *Ptch1*^{DL} mutation on the C57BL/6J background was distinguished from 129S1/SvImJ in the same region using the two sets of primer pairs D13Mit283F (5′- GGA AGC AGT CTC CTG CCT C -3′) with D13Mit283R (5′- GAG AGG TGG CAC ATG AGG TT -3′); and D13mit311F (5′-TGG CTC CTC ATG TTC TAC CC -3′) with D13mit311R (5′-CCA GGT TGT TGC TGC ATT C -3′). PCR was performed using the following parameters: 94°C 12 min; 56 cycles of (94°C 20 sec, 55°C 30 sec, 72°C 45 sec); 72°C 7 min; 4°C hold. Products were resolved on 4% agarose gels and compared to C57BL/6J and 129S1/SvImJ standards. The D13Mit283 primers produce a band of 114bp from C57BL/6J genomic DNA, and a slightly larger band from 129S1/SvImJ. The D13Mit311 primers produce a band of 122bp from C57BL/6J genomic DNA, and a slightly smaller band from 129S1/SvImJ. After the position of the mutation was identified, genotype could be followed using the primers DLF (5′- GGT AAG TCC TTA CTG GTA TCA C -3′) and DLR (5′- CAC CAA ACT GTT CAT TGA TAA AC -3′) for PCR, followed by standard sequence analysis. PCR genotyping for the *Ptch1-LacZ* allele was performed using a protocol provided by the Jackson Laboratory using primers oIMR0204, oIMR0221, oIMR0716, and oIMR0717 (Jax, 2011). *Ptch1*^{mes} and *Ptch1*^{tm1Zim} genotyping was according to protocols recorded in associated publications (Hahn *et al.*, 1998; Makino *et al.*, 2001). Heterozygous *Ptch*^{DL} mice will be made available to the research community upon acceptance of the manuscript.

Skeletal staining

Skeletal staining with alcian blue (Sigma A3157) and alizarin red (Sigma A5533) was performed as described previously (Brewer *et al.*, 2004). Briefly, embryos at 18.5 days post coitum (E18.5) were fixed in 95% ethanol at room temperature for 3 days and stained by

0.15% alcian blue and 0.005% alizarin red for 24 hours. Stained embryos were next cleared with 2% KOH and stored in 50% glycerol until photographed.

Reverse transcription-PCR (RT-PCR)

A detailed RT-PCR protocol was described previously (Feng and Williams, 2003). Briefly, 1ug of total RNA from limb was reverse transcribed into cDNA with SuperScript III (Invitrogen, Cat# 18080-093). Resulting cDNA was used to perform PCR using the AccuPrime Taq DNA polymerase System (Invitrogen, Cat# 12339-016). The primers used to amplify *Ptch1* cDNA were Pt2F (5′- GCA TTC AGT GAA ACA GGA CAG AAT AAG AG -3′) and Pt2R (5′- CGT CTC TCA CTC GGG TGG TCC CAT AAA GG – 3′). PCR was performed using the following parameters: 94 °C 3 min; 35 cycles of (94°C 45 sec, 56°C 45 sec, 68°C 1 min); 68°C 10 min and 4°C hold.

Acknowledgments

We thank Dr. Vida Melvin for valuable comments on the manuscript. We also thank Lori Bulwith, Dr. Lei Zhang, Dr. Martin G. Hanson and Dr. Jian Huang for their involvement in the ENU mutagenesis screen, and Dr. Monica Justice for the gift of mutagenized male mice. We appreciate technical support from V. Bleu Knight for performing the genomic scan to identify the chromosomal region containing the *Ptch1*^{DL} mutation. Funding from a Cancer Center Support Grant (P30CA046934) was used for our sequence analyses and we thank members of this core for their assistance. This research was also supported by National Institutes of Health Grants DE019843 (T.W.) and DE014181 (D.E.C). L.N. is an Investigator of the Howard Hughes Medical Institute.

Funding: This research was also supported by National Institutes of Health Grants DE019843 (T.W.) and DE014181 (D.E.C). L.N. is an Investigator of the Howard Hughes Medical Institute. Sequence analysis was performed using funding from a Cancer Center Support Grant (P30CA046934).

References

Abzhanov A, Rodda SJ, McMahon AP, Tabin CJ. Regulation of skeletogenic differentiation in cranial dermal bone. Development. 2007; 134:3133–3144. [PubMed: 17670790]

Babbs C, Furniss D, Morriss-Kay GM, Wilkie AO. Polydactyly in the mouse mutant Doublefoot involves altered Gli3 processing and is caused by a large deletion in cis to Indian hedgehog. Mechanisms of development. 2008; 125:517–526. [PubMed: 18272352]

Balczerski B, Zakaria S, Tucker AS, Borycki AG, Koyama E, Pacifici M, Francis-West P. Distinct spatiotemporal roles of hedgehog signalling during chick and mouse cranial base and axial skeleton development. Developmental biology. 2012; 371:203–214. [PubMed: 23009899]

Barnes EA, Kong M, Ollendorff V, Donoghue DJ. Patched1 interacts with cyclin B1 to regulate cell cycle progression. EMBO J. 2001; 20:2214–2223. [PubMed: 11331587]

Brewer S, Feng W, Huang J, Sullivan S, Williams T. Wnt1-Cre-mediated deletion of AP-2alpha causes multiple neural crest-related defects. Dev Biol. 2004; 267:135–152. [PubMed: 14975722]

Bruce SJ, Butterfield NC, Metzis V, Town L, McGlinn E, Wicking C. Inactivation of Patched1 in the mouse limb has novel inhibitory effects on the chondrogenic program. The Journal of biological chemistry. 2010; 285:27967–27981. [PubMed: 20576618]

Butterfield NC, Metzis V, Mcglinn E, Bruce SJ, Wainwright BJ, Wicking C. Patched 1 is a crucial determinant of asymmetry and digit number in the vertebrate limb. Development. 2009; 136:3515–3524. [PubMed: 19783740]

Caparros-Martin JA, Valencia M, Reytor E, Pacheco M, Fernandez M, Perez-Aytes A, Gean E, Lapunzina P, Peters H, Goodship JA, Ruiz-Perez VL. The ciliary Evc/Evc2 complex interacts with Smo and controls Hedgehog pathway activity in chondrocytes by regulating Sufu/Gli3 dissociation and Gli3 trafficking in primary cilia. Human molecular genetics. 2013; 22:124–139. [PubMed: 23026747]

Caspary T, Anderson KV. Uncovering the uncharacterized and unexpected: unbiased phenotype-driven screens in the mouse. Dev Dyn. 2006; 235:2412–2423. [PubMed: 16724327]

Christopher KJ, Wang B, Kong Y, Weatherbee SD. Forward genetics uncovers Transmembrane protein 107 as a novel factor required for ciliogenesis and Sonic hedgehog signaling. Developmental biology. 2012; 368:382–392. [PubMed: 22698544]

Cobourne MT, Xavier GM, Depew M, Hagan L, Sealby J, Webster Z, Sharpe PT. Sonic hedgehog signalling inhibits palatogenesis and arrests tooth development in a mouse model of the nevoid basal cell carcinoma syndrome. Developmental biology. 2009; 331:38–49. [PubMed: 19394325]

Cui C, Chatterjee B, Francis D, Yu Q, SanAgustin JT, Francis R, Tansey T, Henry C, Wang B, Lemley B, Pazour GJ, Lo CW. Disruption of Mks1 localization to the mother centriole causes cilia defects and developmental malformations in Meckel-Gruber syndrome. Dis Model Mech. 2011; 4:43–56. [PubMed: 21045211]

Dudas M, Kim J, Li WY, Nagy A, Larsson J, Karlsson S, Chai Y, Kaartinen V. Epithelial and ectomesenchymal role of the type I TGF-beta receptor ALK5 during facial morphogenesis and palatal fusion. Developmental biology. 2006; 296:298–314. [PubMed: 16806156]

Ellis T, Smyth I, Riley E, Graham S, Elliot K, Narang M, Kay GF, Wicking C, Wainwright B. Patched 1 conditional null allele in mice. Genesis. 2003; 36:158–161. [PubMed: 12872247]

Evans, GD.; Farndon, PA. Nevoid Basal Cell Carcinoma Syndrome. In: Pagon, RA.; Bird, TD.; Dolan, CR.; Stephens, K., editors. GeneReviews. Seattle (WA): Univrsity of Washington, Seattle; 2010.

Feng W, Williams T. Cloning and characterization of the mouse AP-2 epsilon gene: a novel family member expressed in the developing olfactory bulb. Mol Cell Neurosci. 2003; 24:460–475. [PubMed: 14572467]

Goodrich LV, Milenkovic L, Higgins KM, Scott MP. Altered neural cell fates and medulloblastoma in mouse patched mutants. Science. 1997; 277:1109–1113. [PubMed: 9262482]

Gritli-Linde A. The Etiopathogenesis of Cleft Lip and Cleft Palate:: Usefulness and Caveats of Mouse Models. Current topics in developmental biology. 2008; 84:37–138. [PubMed: 19186243]

Hahn H, Wojnowski L, Zimmer AM, Hall J, Miller G, Zimmer A. Rhabdomyosarcomas and radiation hypersensitivity in a mouse model of Gorlin syndrome. Nat Med. 1998; 4:619–622. [PubMed: 9585239]

Hayes C, Lyon MF, Morriss-Kay GM. Morphogenesis of Doublefoot (Dbf), a mouse mutant with polydactyly and craniofacial defects. Journal of anatomy. 1998; 193(Pt 1):81–91. [PubMed: 9758139]

Holmes G. The role of vertebrate models in understanding craniosynostosis. Child's nervous system : ChNS : official journal of the International Society for Pediatric Neurosurgery. 2012; 28:1471–1481.

Hurst JA, Jenkins D, Vasudevan PC, Kirchhoff M, Skovby F, Rieubland C, Gallati S, Rittinger O, Kroisel PM, Johnson D, Biesecker LG, Wilkie AO. Metopic and sagittal synostosis in Greig cephalopolysyndactyly syndrome: five cases with intragenic mutations or complete deletions of GLI3. European journal of human genetics : EJHG. 2011; 19:757–762. [PubMed: 21326280]

Iwanaga S, Shimoura H, Shimizu M, Numaguchi Y. Gorlin syndrome: unusual manifestations in the sella turcica and the sphenoidal sinus. AJNR American journal of neuroradiology. 1998; 19:956–958. [PubMed: 9613520]

Jax. 2011. Protocol for genotyping: http://jaxmice.jax.org/protocolsdb/f?p=116:2:1406893156903556::NO:2:P2_MASTER_PROTOCOL_ID,P2_JRS_CODE:1687,003081. In

Jenkins D, Seelow D, Jehee FS, Perlyn CA, Alonso LG, Bueno DF, Donnai D, Josifova D, Mathijssen IM, Morton JE, Orstavik KH, Sweeney E, Wall SA, Marsh JL, Nurnberg P, Passos-Bueno MR, Wilkie AO. RAB23 mutations in Carpenter syndrome imply an unexpected role for hedgehog signaling in cranial-suture development and obesity. American journal of human genetics. 2007; 80:1162–1170. [PubMed: 17503333]

Jiang X, Iseki S, Maxson RE, Sucov HM, Morriss-Kay GM. Tissue origins and interactions in the mammalian skull vault. Developmental biology. 2002; 241:106–116. [PubMed: 11784098]

Johnson DR. Extra-toes: anew mutant gene causing multiple abnormalities in the mouse. J Embryol Exp Morphol. 1967; 17:543–581. [PubMed: 6049666]

Kimonis VE, Goldstein AM, Pastakia B, Yang ML, Kase R, DiGiovanna JJ, Bale AE, Bale SJ. Clinical manifestations in 105 persons with nevoid basal cell carcinoma syndrome. Am J Med Genet. 1997; 69:299–308. [PubMed: 9096761]

Kimonis VE, Singh KE, Zhong R, Pastakia B, Digiovanna JJ, Bale SJ. Clinical and radiological features in young individuals with nevoid basal cell carcinoma syndrome. Genetics in medicine : official journal of the American College of Medical Genetics. 2013; 15:79–83. [PubMed: 22918513]

Klopocki E, Lohan S, Brancati F, Koll R, Brehm A, Seemann P, Dathe K, Stricker S, Hecht J, Bosse K, Betz RC, Garaci FG, Dallapiccola B, Jain M, Muenke M, Ng VC, Chan W, Chan D, Mundlos S. Copy-number variations involving the IHH locus are associated with syndactyly and craniosynostosis. American journal of human genetics. 2011; 88:70–75. [PubMed: 21167467]

Kuijper S, Beverdam A, Kroon C, Brouwer A, Candille S, Barsh G, Meijlink F. Genetics of shoulder girdle formation: roles of Tbx15 and aristaless-like genes. Development. 2005; 132:1601–1610. [PubMed: 15728667]

Lenton, K.; James, AW.; Manu, A.; Brugmann, SA.; Birker, D.; Nelson, ER.; Leucht, P.; Helms, JA.; Longaker, MT. Genesis. New York, NY: 2011. Indian hedgehog positively regulates calvarial ossification and modulates bone morphogenetic protein signaling; p. 2000

Leonardi R, Caltabiano M, Lo Muzio L, Gorlin RJ, Bucci P, Pannone G, Canfora M, Sorge G. Bilateral hyperplasia of the mandibular coronoid processes in patients with nevoid basal cell carcinoma syndrome: an undescribed sign. American journal of medical genetics. 2002; 110:400–403. [PubMed: 12116218]

Lindstrom E, Shimokawa T, Toftgard R, Zaphiropoulos PG. PTCH mutations: distribution and analyses. Human mutation. 2006; 27:215–219. [PubMed: 16419085]

Lo Muzio L. Nevoid basal cell carcinoma syndrome (Gorlin syndrome). Orphanet journal of rare diseases. 2008; 3:32. [PubMed: 19032739]

Mai S, Wei K, Flenniken A, Adamson SL, Rossant J, Aubin JE, Gong SG. The missense mutation W290R in Fgfr2 causes developmental defects from aberrant IIIb and IIIc signaling. Dev Dyn. 2010; 239:1888–1900. [PubMed: 20503384]

Mak KK, Bi Y, Wan C, Chuang PT, Clemens T, Young M, Yang Y. Hedgehog signaling in mature osteoblasts regulates bone formation and resorption by controlling PTHrP and RANKL expression. Dev Cell. 2008; 14:674–688. [PubMed: 18477451]

Mak KK, Chen MH, Day TF, Chuang PT, Yang Y. Wnt/beta-catenin signaling interacts differentially with Ihh signaling in controlling endochondral bone and synovial joint formation. Development. 2006; 133:3695–3707. [PubMed: 16936073]

Makino S, Masuya H, Ishijima J, Yada Y, Shiroishi T. A spontaneous mouse mutation, mesenchymal dysplasia (mes), is caused by a deletion of the most C-terminal cytoplasmic domain of patched (ptc). Dev Biol. 2001; 239:95–106. [PubMed: 11784021]

Matsumaru D, Haraguchi R, Miyagawa S, Motoyama J, Nakagata N, Meijlink F, Yamada G. Genetic analysis of Hedgehog signaling in ventral body wall development and the onset of omphalocele formation. PloS one. 2011; 6:e16260. [PubMed: 21283718]

McBratney-Owen B, Iseki S, Bamforth SD, Olsen BR, Morriss-Kay GM. Development and tissue origins of the mammalian cranial base. Developmental biology. 2008; 322:121–132. [PubMed: 18680740]

Meester-Smoor MA, Vermeij M, van Helmond MJL, Molijn AC, van Wely KHM, Hekman ACP, Vermey-Keers C, Riegman PHJ, Zwarthoff EC. Targeted disruption of the Mn1 oncogene results in severe defects in development of membranous bones of the cranial skeleton. Molecular and Cellular Biology. 2005; 25:4229–4236. [PubMed: 15870292]

Milenkovic L, Goodrich LV, Higgins KM, Scott MP. Mouse patched1 controls body size determination and limb patterning. Development. 1999; 126:4431–4440. [PubMed: 10498679]

Nagayama M, Iwamoto M, Hargett A, Kamiya N, Tamamura Y, Young B, Morrison T, Takeuchi H, Pacifici M, Enomoto-Iwamoto M, Koyama E. Wnt/beta-catenin signaling regulates cranial base development and growth. Journal of Dental Research. 2008; 87:244–249. [PubMed: 18296608]

Ngan ES, Garcia-Barcelo MM, Yip BH, Poon HC, Lau ST, Kwok CK, Sat E, Sham MH, Wong KK, Wainwright BJ, Cherny SS, Hui CC, Sham PC, Lui VC, Tam PK. Hedgehog/Notch-induced

premature gliogenesis represents a new disease mechanism for Hirschsprung disease in mice and humans. The Journal of clinical investigation. 2011; 121:3467–3478. [PubMed: 21841314]

Ohba S, Kawaguchi H, Kugimiya F, Ogasawara T, Kawamura N, Saito T, Ikeda T, Fujii K, Miyajima T, Kuramochi A, Miyashita T, Oda H, Nakamura K, Takato T, Chung Ui. Patched1 haploinsufficiency increases adult bone mass and modulates Gli3 repressor activity. Developmental cell. 2008; 14:689–699. [PubMed: 18477452]

Pacheco M, Valencia M, Caparros-Martin JA, Mulero F, Goodship JA, Ruiz-Perez VL. Evc works in chondrocytes and osteoblasts to regulate multiple aspects of growth plate development in the appendicular skeleton and cranial base. Bone. 2012; 50:28–41. [PubMed: 21911092]

Quijada, L.; Callejo, A.; Torroja, C.; Guerrero, I. The Patched Receptor: Switching On/Off the Hedgehog Signaling Pathway. In: Ruiz i Altaba, A., editor. Hedgehog-gli signaling in human disease. Austin, Tx: Landes Bioscience; 2006.

Reid BS, Yang H, Melvin VS, Taketo MM, Williams T. Ectodermal Wnt/beta-catenin signaling shapes the mouse face. Developmental biology. 2011; 349:261–269. [PubMed: 21087601]

Rice DP, Connor EC, Veltmaat JM, Lana-Elola E, Veistinen L, Tanimoto Y, Bellusci S, Rice R. Gli3Xt-J/Xt-J mice exhibit lambdoid suture craniosynostosis which results from altered osteoprogenitor proliferation and differentiation. Human molecular genetics. 2010; 19:3457–3467. [PubMed: 20570969]

Robbins DJ, Fei DL, Riobo NA. The Hedgehog signal transduction network. Science signaling. 2012; 5:re6. [PubMed: 23074268]

Roberts RB, Hu Y, Albertson RC, Kocher TD. Craniofacial divergence and ongoing adaptation via the hedgehog pathway. Proc Natl Acad Sci U S A. 2011; 108:13194–13199. [PubMed: 21788496]

St-Jacques B, Hammerschmidt M, McMahon AP. Indian hedgehog signaling regulates proliferation and differentiation of chondrocytes and is essential for bone formation. Genes & development. 1999; 13:2072–2086. [PubMed: 10465785]

Sweet HO, Bronson RT, Donahue LR, Davisson MT. Mesenchymal dysplasia: a recessive mutation on chromosome 13 of the mouse. The Journal of heredity. 1996; 87:87–95. [PubMed: 8830098]

Wakabayashi Y, Mao JH, Brown K, Girardi M, Balmain A. Promotion of Hras-induced squamous carcinomas by a polymorphic variant of the Patched gene in FVB mice. Nature. 2007; 445:761–765. [PubMed: 17230190]

Weatherbee SD, Niswander LA, Anderson KV. A mouse model for Meckel syndrome reveals Mks1 is required for ciliogenesis and Hedgehog signaling. Human molecular genetics. 2009; 18:4565–4575. [PubMed: 19776033]

Wicking C, Shanley S, Smyth I, Gillies S, Negus K, Graham S, Suthers G, Haites N, Edwards M, Wainwright B, Chenevix-Trench G. Most germ-line mutations in the nevoid basal cell carcinoma syndrome lead to a premature termination of the PATCHED protein, and no genotype-phenotype correlations are evident. American journal of human genetics. 1997; 60:21–26. [PubMed: 8981943]

Winnier GE, Hargett L, Hogan BL. The winged helix transcription factor MFH1 is required for proliferation and patterning of paraxial mesoderm in the mouse embryo. Genes & development. 1997; 11:926–940. [PubMed: 9106663]

Yang Y, Guillot P, Boyd Y, Lyon MF, McMahon AP. Evidence that preaxial polydactyly in the Doublefoot mutant is due to ectopic Indian Hedgehog signaling. Development. 1998; 125:3123–3132. [PubMed: 9671585]

Young B, Minugh-Purvis N, Shimo T, St-Jacques B, Iwamoto M, Enomoto-Iwamoto M, Koyama E, Pacifici M. Indian and sonic hedgehogs regulate synchondrosis growth plate and cranial base development and function. Developmental biology. 2006; 299:272–282. [PubMed: 16935278]

Yuksel-Apak M, Bogershausen N, Pawlik B, Li Y, Apak S, Uyguner O, Milz E, Nurnberg G, Karaman B, Gulgoren A, Grzeschik KH, Nurnberg P, Kayserili H, Wollnik B. A large duplication involving the IHH locus mimics acrocallosal syndrome. European journal of human genetics : EJHG. 2012; 20:639–644. [PubMed: 22234151]

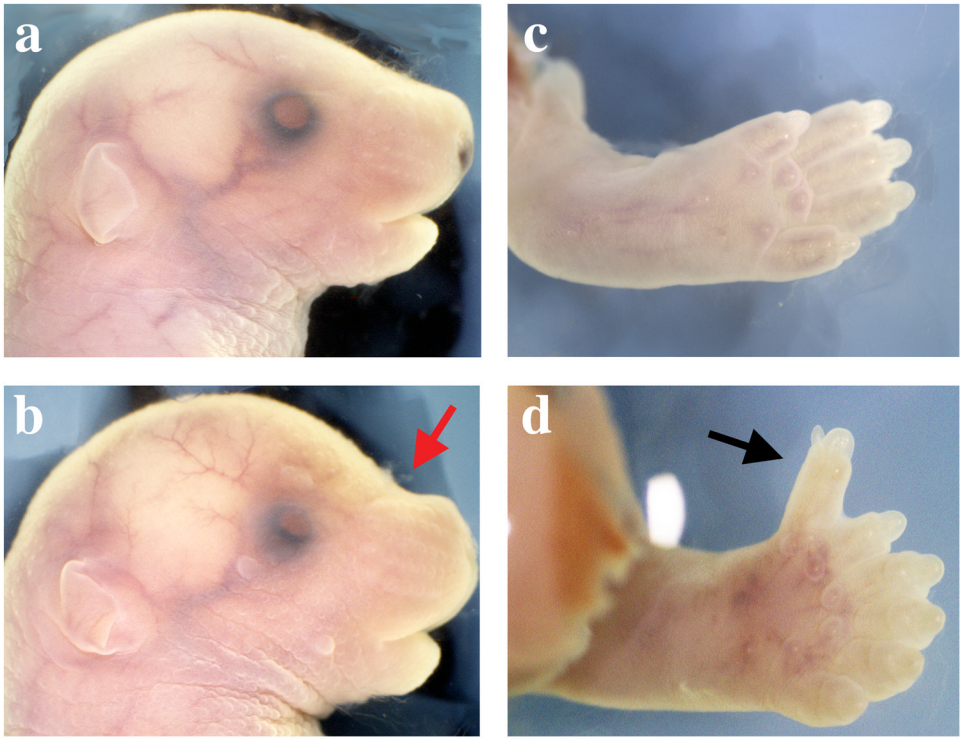

Figure 1.
Gross external developmental defects in the *Ptch1*^{DL} homozygous mutants.
E18.5 wild type (a, c) and *Ptch1*^{DL} mutants (b, d) showing abnormal flexure at skull and nasal juncture (red arrow, b) and forelimb preaxial polydactyly (black arrow, d).

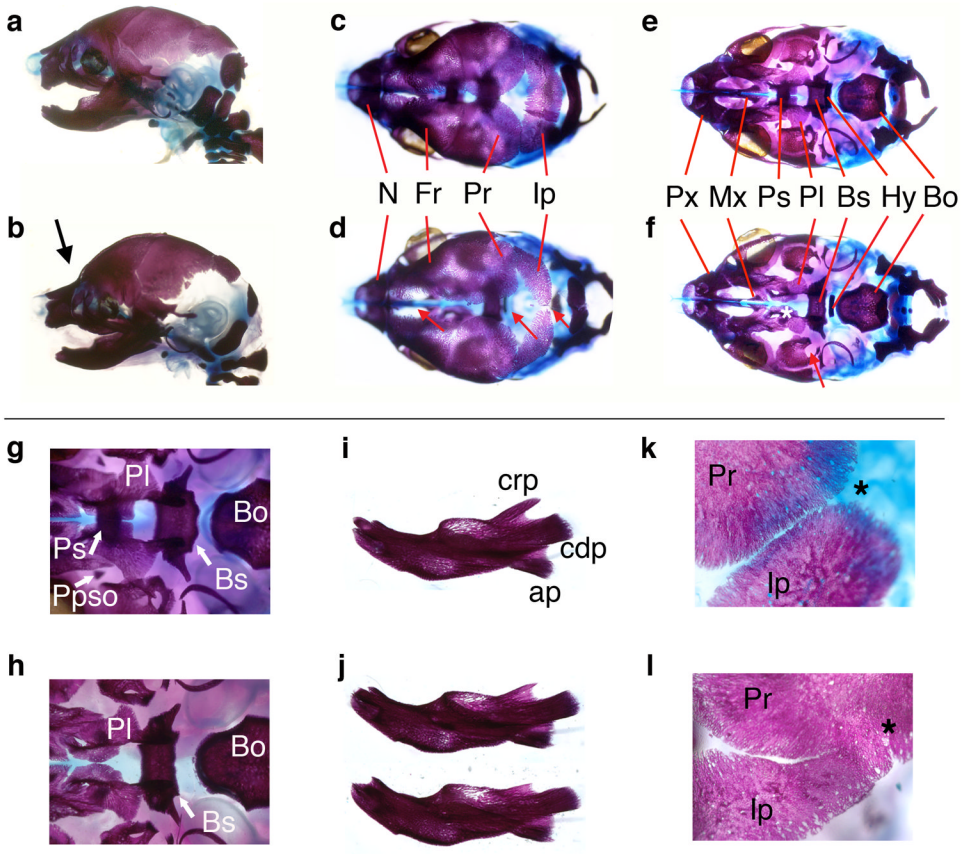

Figure 2.

Craniofacial skeletal abnormalities in *Ptch1*^{DL} homozygous mutants.

E18.5 control (a, c, e, g, i, k) and *Ptch1*^{DL} mutant skulls (b, d, f, h, j, l) shown in lateral (a, b), dorsal (c, d) and ventral views with mandibles removed (e-h). (g) and (h) show detail of cranial base with hyoid bone removed. (Note that the pila postopitca (Ppso), which forms a component of the orbitosphenoid, was occasionally present in the mutants. It can also be absent in control embryos at this stage). (i, j) lateral views of control dentary bone (i) and dentary bones from two separate *Ptch1*^{DL} mutants (j). (k, l) show detail of lambdoid suture between parietal and interparietal bones. Midline is to left and lateral to right. Asterisk shows expected junction between bones.

Key. (b) Abnormal flexure at skull and nasal juncture is shown by a black arrow. (d) Red arrows demonstrate delayed or abnormal development of the bones of the cranial vault in the midline in *Ptch1*^{DL} mutants. (f) White asterisk highlights the absence of the presphenoid bone and the underdevelopment of the palatal shelves, red arrow shows the abnormal morphology of the alisphenoid bone in *Ptch1*^{DL} mutants. Bo, basioccipital; Bs, basisphenoid; cdp, condylar process; crp, coronoid process; Fr, frontal bone; Hy, hyoid; Ip, interparietal bone; Mx, palatine process of the maxilla; N, nasal bone; Pl, palatine; Ppso, pila postoptica; Pr, parietal bone; Ps, presphenoid; Px, premaxilla.

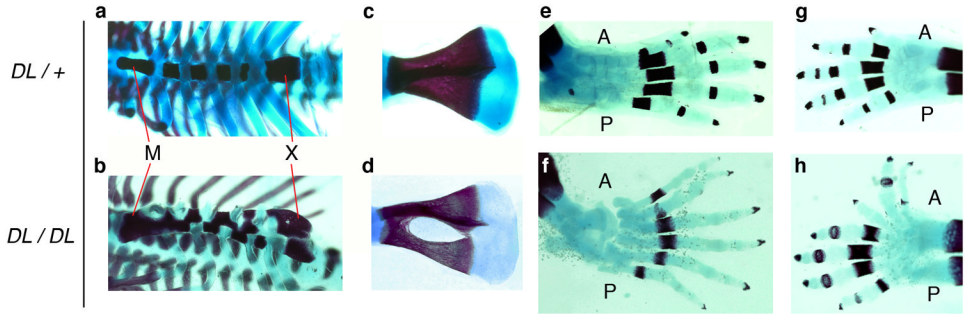

Figure 3.

Additional skeletal abnormalities in *Ptch1*^{DL} homozygous mutants.

E18.5 wild-type (a, c, e, g) and *Ptch1*^{DL} mutants (b, d, f, h) showing ribcage in ventral view (a, b), scapula (c, d), hindlimb (e, f) and forelimb (g, h). Note the ribs have been cut by the investigators on one side of the sternum in the mutant sample. A, anterior; M, manubrium; P, posterior; X, xiphoid process.

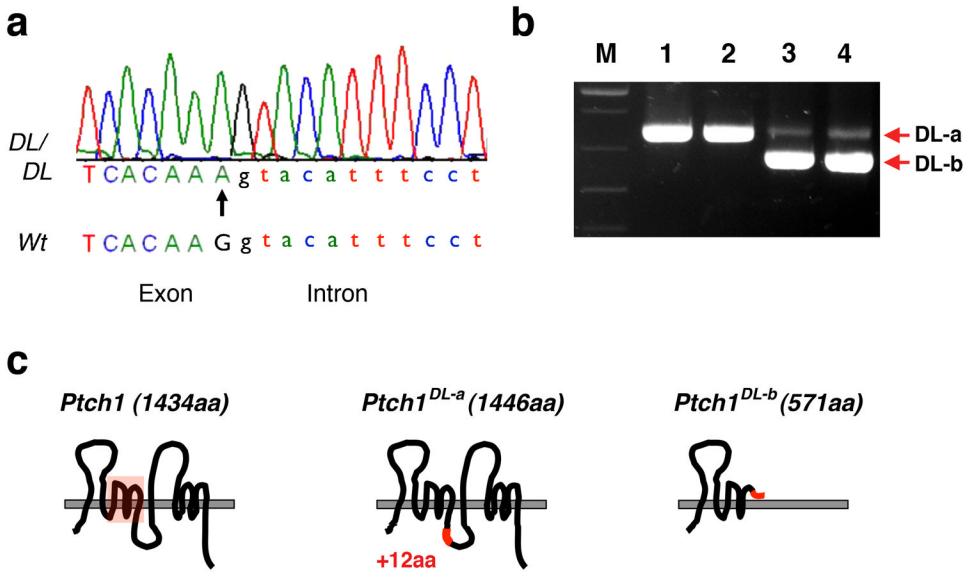

Figure 4.

Ptch1^{DL} harbors a point mutation in *Ptch1*. (a) Chromatograph sequencing result for *Ptch1*^{DL} mutant showing *Ptch1* genomic sequences at the junction of exon 13 and intron 13. The G to A point mutation in the *Ptch1*^{DL} mutant is labeled with an arrow. (b) RT-PCR results for wild-type (lanes 1 and 2) and *Ptch1*^{DL} mutant embryos (lanes 3 and 4) obtained using *Ptch1* primers Pt2F and Pt2R. "M" = markers. (c) Graphic representation of wild-type Ptch1 protein and two putative Ptch1 proteins based on their mRNA sequences in *Ptch1*^{DL} mutant embryos. The sterol sensing domain is shown by the red box in the wild-type protein. The DL-a form changes the normal sequence from DIFCC FTSPC VSRVI to DIFCC FTKYI SWCLG PVFFG PCVSR VI i.e. the addition of 36 nucleotides, with a new in-frame splice at a GGGT donor sequence, the change of S to K followed by the addition of 12 new amino acids. The DL-b form changes the normal sequence from FSLQA AVVVV FN to FSLQP LCQQG DSS* as exon 13, which has the mutated splice donor sequence, is skipped. The resulting splice from exon 12 to 14 is out of frame and creates a premature stop codon after 9 amino acids.

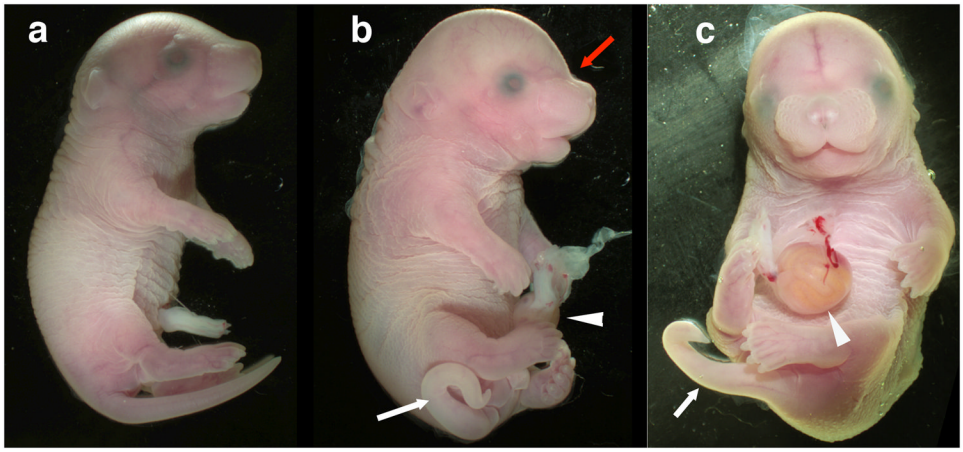

Figure 5.

Allelic non-complementation between *Ptch1*^{DL} and *Ptch1*^{tm1Zim} at E18.5.

Whole mount images of wild-type (a) and two *Ptch1*^{DL}/*Ptch1*^{tm1Zim} embryos (b, c) in lateral (a, b) or ventral (c) view. In the mutant embryos, the kinked tail (white arrow), omphalocele (white arrowhead) and abnormal skull shape (red arrow) are illustrated.

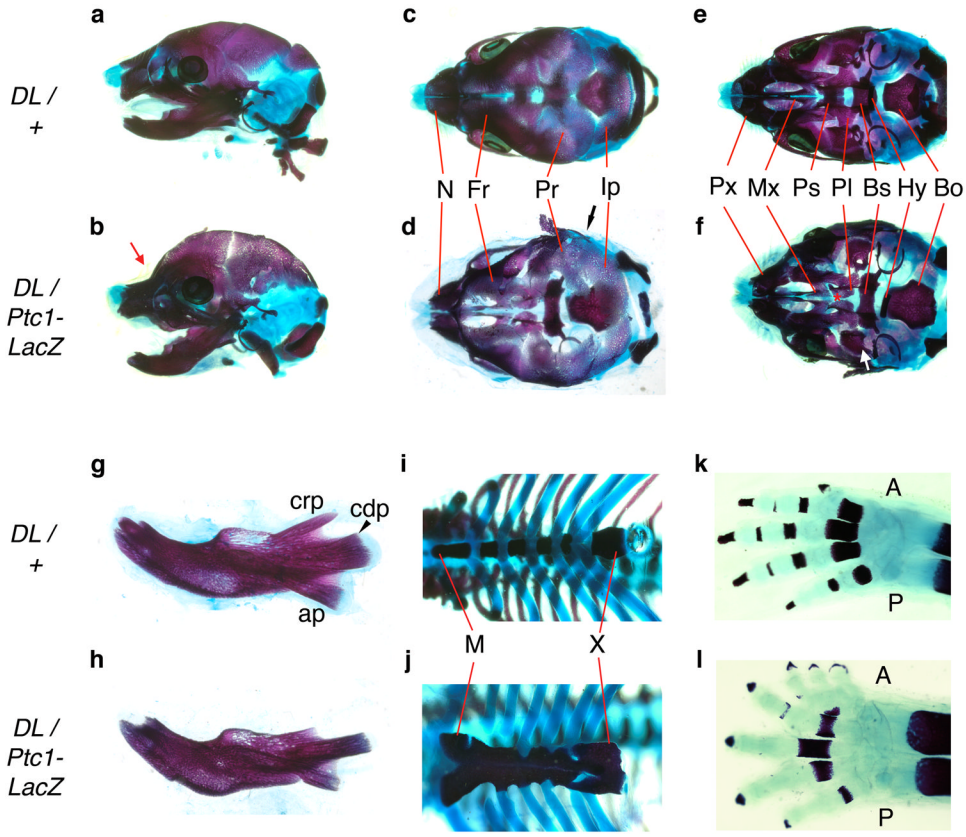

Figure 6.

Skeletal staining illustrating non-complementation between *Ptch1*^{DL} and *Ptch1-LacZ* mutant alleles.

E18.5 *Ptch1*^{DL} heterozygotes (a, c, e, g, i, k) and *Ptch1*^{DL}*/Ptch1-LacZ* mutants (b, d, f, h, j, l). Lateral views of skulls (a, b) with red arrow showing abnormal flexure at skull and nasal juncture. Dorsal view of skulls (c, d). Black arrow in (d) illustrates lack of lambdoid suture. Ventral view of skull with mandibles removed (e, f) with the absence of the presphenoid bone and the underdevelopment of the palatal shelves (red asterisk), and the aberrant morphology of the alisphenoid bone (white arrow) marked in the *Ptch1*^{DL}*/Ptch1-LacZ* mutants. (g, h) Lateral view of dentary bones. (i, j) Ribcage in ventral view. (k, l) forelimbs. Key: A, anterior; ap, angular process; Bo, basioccipital; Bs, basisphenoid; cdp, condylar process; crp, coronoid process; Fr, frontal bone; Hy, hyoid; Ip, interparietal bone; M, manubrium; Mx, palatine process of the maxilla; N, nasal bone; P, posterior; Pl, palatine; Pr, parietal bone; Ps, presphenoid; Px, premaxilla; X, xiphoid process.

Table 1

Phenotypes of *Ptch*^{DL} homozygous mice and negative complementation with the *Ptch1*^{null} allele.

Phenotype[*]	**Genotype *DL/DL***	***+/+ and DL/+ and Ptch1-LacZ/+***	***DL/Ptch1-LacZ***
Dead	0	0	17
Exencephaly	0	0	34
Skull vault hypoplasia	100	0	100
Lambdoid suture synostosis	100	0	100[#]
Narrow basisphenoid	100	0	100
Missing presphenoid	100	0	100
Hypoplastic alisphenoid	100	0	100
Hypoplastic palatal shelves	100	0	100
Coronoid hypoplastic	37.5	0	100
Kinked Tail	0	0	34
Abnormal sternum	100	0	100[$]
Defective scapulas	12.5	0	50
Affected forelimbs	100	0	100
Affected hindlimbs	100	0	78

[*] Numbers represent the percentage of a particular genotype showing an abnormal phenotype for the structure described.

[#] Lambdoid suture synostosis was only scored in *DL/Ptch1-LacZ* embryos that underwent normal neural tube closure and had sufficient development of the calvaria for visualization.

[$] Bifurcated and fused ribs occur in association with sternal defects in some embryos.